Quantum description of the hindered rotor motion of CH_4 adsorbed on MgO(100) and He-bound state analysis

S. Picaud and C. Girardet*
Laboratoire de Physique Moléculaire–UMR CNRS 6624, Faculté des Sciences, La Bouloie, Université de Franche-Comté, 25030 Besançon Cedex, France

T. Duhoo and D. Lemoine
Laboratoire de Physique des Lasers, Atomes et Molécules–UMR CNRS, Université des Sciences et Technologie de Lille, Bâtiment P5, 59655 Villeneuve d'Ascq Cedex, France

(Received 5 January 1999)

Within a semiempirical potential strategy we compare a $T=0$ K classical determination of the structure of the CH_4 monolayer with a finite temperature quantum mechanical treatment of the orientational motions of the tetrahedral molecules in the layer. In the classical model, the molecules adopt a tripod configuration at a distance 2.74 Å from the surface, with an adsorption energy per molecule E_A equal to -228 meV. In the quantum approach, the nearly uncorrelated orientational motions of the admolecules at a distance of -2.95 Å from the surface look like those of a hindered rotor with large amplitude angular motions. The corresponding value of the adsorption energy $E_A=-152$ meV is close to the experimental isosteric heat of adsorption (-145 ± 10 meV). In addition, the calculated energies of bound states for He atoms trapped near a methane-plated MgO system indicate upon comparison with scattering experiments, that helium atoms could probe an orientational quantum CH_4 layer and not a frozen equilibrium structure, even at very low temperature. [S0163-1829(99)01335-1]

I. INTRODUCTION

First concentrated in the seventies on hexagonal substrates such as graphite,[1–3] the studies of adsorption of two-dimensional methane films were then extended in the last decade to square ionic lattices, namely the (100) surfaces of MgO (Ref. 4–18) and NaCl.[19,20] Experimental determinations of the CH_4 monolayer structure were done using low energy electron diffraction, neutron scattering,[4–9,18] helium atom scattering[10,11] (HAS) and polarized infrared spectroscopy,[17,19,20] whereas measurements of the adsorption energy were obtained from thermodynamics[16] and desorption experiments.[11] On MgO(100), methane was shown to form an ordered $c(\sqrt{2}\times\sqrt{2})R45°$ structure at low temperature,[4] and a two-dimensional liquid phase above 85 K.[5] The heat of adsorption estimated from volumetric isotherms is equal to 13.1 kJ/mol,[16] a value that agrees well with desorption measurements.[11] On NaCl(100), CH_4 accomodates rather a (1×1) monolayer at 45 K whereas a $p(2\times2)$ structure was observed at lower temperature. This latter geometry evolves toward a (1×1) phase after about two hours as the probable result of nuclear spin conversion.[20] The heat of adsorption measured at submonolayer coverage on NaCl(100) is the same as on MgO(100).[19]

However several questions concerning the orientational and translational dynamics of the CH_4 molecules on the surface remained partially answered, only. On NaCl, an analysis of the infrared spectra[20] tended to privilege a dipod configuration for the admolecules (i.e., two hydrogen atoms pointing towards the surface) but a tripod orientation with three hydrogens pointing towards the surface could not be excluded, in the case where the molecules perform free cogwheeling on the surface.[19] On MgO, inelastic neutron and helium probes were extensively used to measure the dynamics and kinetics of CH_4 at various temperatures. At high temperature (70 K), quasielastic neutron scattering experiments[9] showed that the monolayer is solid, the rotation of the molecules being isotropic and their center of mass being trapped at their lattice sites. The diffusion constant was measured for the liquid film around 90 K and shown to be lower by two orders of magnitude than on graphite, indicating significant corrugation on the MgO substrate. Rotational diffusion on the CH_4 monolayer was then studied[9] between 20 and 50 K, which evidenced isotropic rotation of methane molecules above 40 K, and intermediate motions between free rotor and rotation around a twofold axis perpendicular to the surface for $T<40$ K. Rotational tunneling of methane on MgO(100) was examined at very low temperature ($T\sim4$ K) by inelastic neutron scattering,[8] which concluded to a dipod orientation of CH_4. Recent experiments[18] at even lower temperature ($T=1.5$ K) compared the high-resolution inelastic neutron tunneling spectrum of the CH_4 monolayer with the multilayer one. They corroborated the trend for a dipod orientation on the basis of symmetry arguments applied to tunneling data at 1.5 K, while the spectrum broadened gradually until molecular rotational diffusion was evidenced at 15 K. The results of HAS measurements at T around 30 and 40 K could also be interpreted[10] on the basis of free rotation of CH_4 molecules at their adsorption sites. An Einstein-like vibrational mode was found at 7.5 meV in time-of-flight spectrum. Finally, the polarization infrared spectra of CH_4 adsorbed on MgO(100) at $T=40$ K appreciably differed from those observed on NaCl(100), and were preferentially interpreted on the basis of free rotating molecules.[17]

The question about the preferred orientation of methane molecules on the (100) MgO surface was also addressed theoretically. Molecular-dynamics simulations[12] and 0 K equilibrium calculations[13] using semiempirical potentials

showed that the tripod orientation for the molecules was much more stable than the dipod one. For the monolayer, two structures characterized by different tripod orientations of the molecules were found[12] to have nearly the same stability and the lack of energy barrier between these structures was interpreted as the signature of a possible free cogwheeling CH_4 motion. However, the calculated energy per molecule (23 kJ/mol) was strongly overestimated when compared to the experimental value (13.1 kJ/mol). Earlier *ab initio* calculations[14] favored the dipod-down configuration for the CH_4/MgO(100) system. The results of quantum chemical approach were recently revisited on the basis of high-level *ab initio* potentials, in conjunction with embedded cluster model.[15] It was shown that the dipod orientation for a single methane molecule is slightly more stable by 0.8 kJ/mol than the tripod configuration. This trend was confirmed in the monolayer, but the surprinsingly low value (8.5 kJ/mol) of the calculated total adsorption energy per molecule compared to the experimental one, could let some suspicions on the accuracy of the dipod versus tripod energy difference.

In this paper, we investigate theoretically the adsorption of CH_4 on MgO on the basis of a quantum description of the orientational motions of the admolecules. Such an approach was recently used to characterize the adsorption of quantum layers (H_2, D_2) on NaCl,[21] and it is expected to be necessary for the study of molecules characterized by small mass and large rotational constant when the substrate corrugation remains small. Semiempirical potentials for the CH_4–MgO system are used to compare the adsorption characteristics in the classical and quantum approaches. These results allow us to calculate the bound states of helium atoms impinging on the CH_4 monolayer, using a quantum description of the He/CH_4 collisional process. This calculation serves as a probe of the monolayer geometry since the bound states can be directly compared to the experimental HAS data.[10]

The organization of the paper is as follows: In Sec. II, we present the study of the adsorption characteristics on the basis of both classical and quantum approaches. Section III is devoted to the determination of the bound-state energies for He/CH_4/MgO. The discussion of the results and the comparison with theoretical and experimental studies are given in Sec IV.

II. DETERMINATION OF THE ADSORPTION CHARACTERISTICS

A. Interaction potential

The molecule–substrate potential V_{MS} is written as a sum of two main contributions: the pairwise atom-atom Lennard-Jones interactions describing the dispersion-repulsion contribution V_{MS}^{DR}, and the electrostatic terms V_{MS}^{E} characterizing the interaction between the multipole moments of CH_4 and the strong electric field of the MgO surface created by the charges $q_{Mg}=-q_O=1.2$ e.[22] Due to the T_d symmetry of the CH_4 molecule, the first non-zero electric moment is the octopole, which is schematized, within the distributed multipole analysis approach, by five charges distributed on the C and H atoms ($q_C=-0.572$ e and $q_H=+0.143e$).[12] To ensure the convergence of V_{MS}^{E} for the electrostatic interaction, the charge–charge term is expanded in the two-dimensional reciprocal space of the MgO surface. In addition, the induction interaction V_{MS}^{I} accounts for the polarization of the molecule, with polarizability[23] $\alpha_{CH_4}=2.6$ Å^3, by the electric field of the substrate. The lateral interactions V_{MM} between CH_4 molecules are written in the same way as the sum of Lennard-Jones (V_{MM}^{DR}) and of electrostatic (V_{MM}^{E}) interactions between the C and H atoms. Higher terms such as substrate mediated contributions are neglected.

The total interaction potential between the molecules and the surface is then written as

$$V=\sum_i \left\{ V_{MS}^{DR}(\mathbf{R}_i,\mathbf{\Omega}_i)+V_{MS}^{E}(\mathbf{R}_i,\mathbf{\Omega}_i)+V_{MS}^{I}(\mathbf{R}_i,\mathbf{\Omega}_i) + \sum_{j\neq i}\left[V_{MM}^{DR}(\mathbf{R}_i,\mathbf{R_j},\mathbf{\Omega}_i,\mathbf{\Omega}_j)+V_{MM}^{E}(\mathbf{R}_i,\mathbf{R_j},\mathbf{\Omega}_i,\mathbf{\Omega}_j)\right]\right\}, \tag{1}$$

where the positions $\mathbf{R}_i=(x_i,y_i,z_i)$ and the orientations $\mathbf{\Omega}_i=(\theta_i,\phi_i,\chi_i)$ of the ith molecule are referred to an absolute frame tied to the surface.

B. Classical approach

Within the classical approach, the admolecule characteristics (adsorption site and energy, molecular orientation, structure of the adlayer . . .) are determined from the minimization of the potential energy V with respect to the translational and orientational variables of the admolecules. The minimization procedure, based on a conjugate gradient method, has proved to be very accurate for many adsorbate/substrate systems.[24–27]

The single admolecule is adsorbed in a tripod configuration above a Mg site, at a molecule-surface distance $z=2.74$ Å and with an adsorption energy $V=-204$ meV. The dipod configuration above the same adsorption site is much less stable ($V=-149$ meV) and the corresponding equilibrium distance is much larger ($z=2.98$ Å). Note that when the monopod orientation is considered, the molecule is adsorbed between two cations, at the distance $z=3.40$ Å and with an energy equal to -98 meV. At the monolayer completion, the lateral interactions between CH_4 molecules adsorbed on adjacent sites of the (100) surface (distance $a=2.98$ Å) are strongly repulsive. By contrast second nearest-neighbor Mg sites ($a\sqrt{2}=4.21$ Å) accomodate very well attractive interactions between CH_4 since this distance between nearest-neighbor molecules is close to the bulk methane parameter equal to 4.16 Å . Thus, in accordance with neutron diffraction experiments, we consider monolayer structures with a unit cell rotated by 45° with respect to the substrate unit cell, and a density of one CH_4 molecule per two substrate Mg sites.

The relative stability of three different monolayer structures, namely the $(\sqrt{2}\times\sqrt{2})R45°$ (case a), the $(2\sqrt{2}\times\sqrt{2})R45°$ (case b), and the $(2\sqrt{2}\times2\sqrt{2})R45°$ (case c) phases containing one, two and four molecules per unit cell, respectively, has been studied from the potential minimization. For case a, the CH_4 molecule is found to be adsorbed above the Mg site, at $z=2.74$ Å and with the tripod orientation (Fig. 1), exactly as for the single admolecule. The total

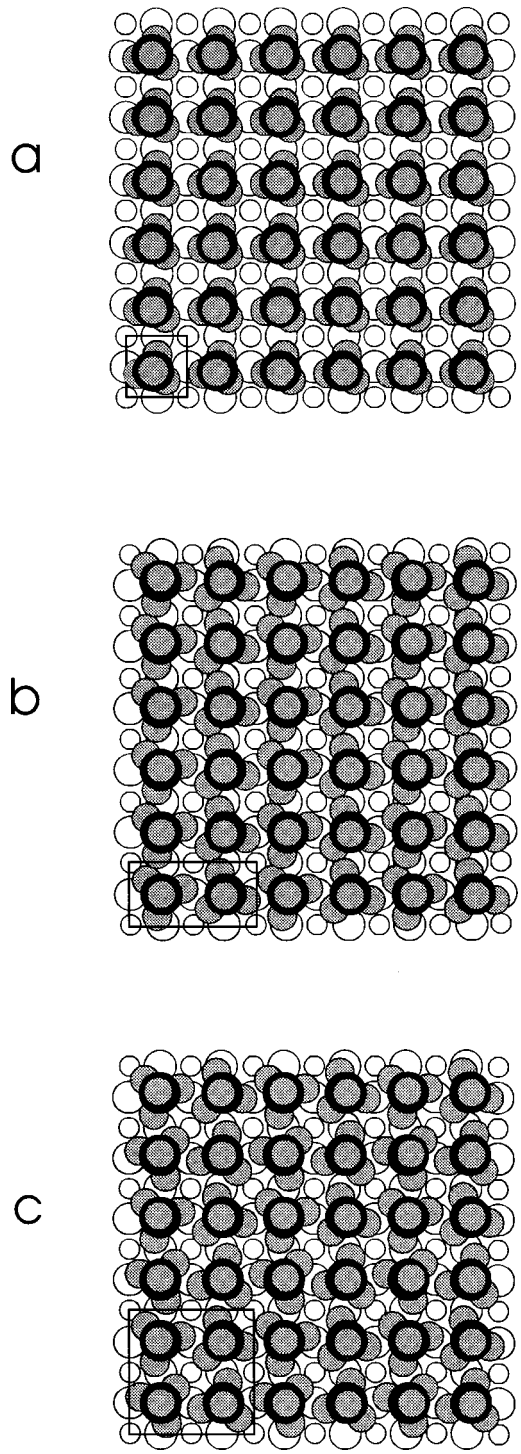

FIG. 1. Geometry of the stable structures for the CH_4 monolayer adsorbed on MgO(100), within the classical approach : $(\sqrt{2}\times\sqrt{2})R45°$ phase containing one molecule per unit cell (a), $(2\sqrt{2}\times\sqrt{2})R45°$ phase containing two molecules per unit cell (b) and $(2\sqrt{2}\times 2\sqrt{2})R45°$ phase containing four molecules per unit cell (c).

energy is equal to -225 meV and the lateral energy represents 9% of the total potential, only. The two other cases (b and c) differ by the relative orientations of the H atoms in the tripod configuration (Fig. 1) and thus by the relative orientations of adjacent molecules. In these two phases the adsorption energy per molecule is the same ($V=-228$ meV). Note a slightly larger contribution of the lateral interaction (11%) in case c balanced by a slightly less stable configuration of the molecules on the surface in case b. Therefore the transition from phase b to phase c should be allowed by a free cogwheeling motion in agreement with the results of Alavi.[12]

We have also performed energy calculations for the same structures containing now molecules in dipod orientation. The most stable dipod structure is the $(2\sqrt{2}\times 2\sqrt{2})R45°$ phase containing four molecules per unit cell at the molecule–surface distance $z=3.03$ Å . The adsorption energy per molecule is equal to -177 meV, only, and it is clearly less stable than the tripod stucture by about 50 meV. Therefore, we conclude that, for the semiempirical potential considered here, the most stable monolayer structures (classical approach) are the $(2\sqrt{2}\times\sqrt{2})R45°$ and the $(2\sqrt{2}\times 2\sqrt{2})R45°$ phases, with two and four molecules per unit cell, respectively, adsorbed on Mg sites with tripod orientations. The barrier to the CH_4 rotation is large (55 meV) and the center of mass of the molecule is strongly trapped at a distance of 2.74 Å from the surface, above the Mg site. The harmonic frequencies connected to the perpendicular vibrations and to the lateral vibrations of the CH_4 center of mass are $\omega_z=129$ and $\omega_x=\omega_y=55$ cm^{-1}, respectively.

C. Quantum approach

Since the methane molecule is characterized by a high symmetry, a relatively light mass $\mu=2.66\times10^{-23}$ g and a large rotational constant $B\equiv\hbar^2/2I=5.25$ cm^{-1},[28] a quantum approach should be more appropriate for the determination of the orientational properties of the adspecies.

1. Single molecule

The total Hamiltonian for an adsorbed rigid CH_4 molecule labeled i is defined as

$$H_i=\frac{P_i^2}{2\mu}+\frac{L_i^2}{2I}+V_{MS}(\mathbf{R}_i,\mathbf{\Omega}_i), \tag{2}$$

where $\mathbf{P}_i$ and $\mathbf{L}_i$ are the linear and angular momenta of CH_4, respectively. We solve the secular equation connected to H_i using an iterative procedure.

First, we consider the CH_4 molecule as a free rotor above the surface with eigenstates $|JMK\rangle$, and we minimize the average potential $\langle JMK|V_{MS}|JMK\rangle$ with respect to z for a sampling of (x,y) positions in order to obtain the potential energy map $\overline{V}_{MS}(x,y)$. This potential energy map (PEM) gives information on the trapping of the molecular center of mass on the surface (site $x^{(0)},y^{(0)},z^{(0)}$) and on the possible diffusion valleys. At this site, we then solve the secular orientational equation connected to H_i by expanding the orientational eigenstates as a linear combination of the free rotor eigenkets, as[21]

$$|jmk\rangle=\sum_{JMK} a_{JMK}^{jmk}|JMK\rangle. \tag{3}$$

The corresponding secular equation is written

$$\sum_{JMK}\sum_{J'M'K'} a_{JMK}^{jmk} a_{J'M'K'}^{j'm'k'\star}[(BJ(J+1)-E^0)\delta_{JJ'}\delta_{MM'}\delta_{KK'} + \langle J'M'K'|V_{MS}(x^{(0)},y^{(0)},z^{(0)},\theta,\phi,\chi))|JMK\rangle] = 0 \tag{4}$$

where $BJ(J+1)$ is the rotational energy of CH_4 in the gas phase. The solutions of Eq. (4) are the new eigenvalues E_{jmk}^0 and eigenkets $|jmk\rangle$ for the admolecule. In principle, this procedure is iterated by considering the new map $\langle jmk|V_{MS}|jmk\rangle$ and determining the new values of x,y, and z until convergence is reached. At each step, we can have information on the translational dynamics of the molecule by solving the part of the Hamiltonian, which depends on the motions x,y, and z of the center of mass around its equilibrium [Eq. (2) after replacing V_{MS} by $\langle V_{MS}\rangle$]. The expansion coefficients in the free rotor basis [Eq. (3)] depend on the symmetry and magnitude of the PEM V_{MS} and also on the shape of the admolecule. The orientational dependence of V_{MS} is consistently expressed in terms of the $D_{p,q}^{\ell}$ Wigner functions.[21] The first nonzero ℓ order is of rank 3 due to the T_d symmetry of CH_4. For a given value J, the Wigner expansion of Eq. (3) implies $(J+1)(4J^2+8J+3)/3$ basis states including the degeneracy on M and K. The expansion was truncated to the upper value $J=6$, yet involving 455 kets of the free rotor basis. Therefore, in practice convergence of the iterative method is rather time consuming.

At the first step of the iteration, i.e., when the molecule behaves as a free rotor, the electrostatic part of V_{MS} vanishes and the remaining term in $\overline{V}_{MS}$ comes mainly from the isotropic part of the dispersion-repulsion interaction. The corresponding potential map $\overline{V}_{MS}=\langle JMK|V_{MS}|JMK\rangle$ drawn in Fig. 2 shows that the stable site is found above a cation $(x^{(0)}=0,y^{(0)}=0)$, for a molecule-surface distance $z^{(0)}=3.18$ Å and an adsorption energy equal to -116 meV. These values are very different from the frozen configurations discussed in Sec. II B. The anion site is significantly less stable since the energy increases up to -89 meV and the distance up to $z=3.49$ Å . The corrugation along the diffusion valley between two consecutive Mg sites is significantly lowered (8.5 meV) when compared to the frozen configurations.

Figure 3 exhibits the orientational levels obtained from the resolution of Eq. (4) after two steps, for which we consider that convergence is reached in analogy with calculations performed in Ref. 21. When compared to the orientational level scheme of the free rotor molecule (left-hand side of Fig. 3), the new level scheme clearly exhibits the influence of the surface through the degeneracy removing of the $|JMK\rangle$ levels, leading to a splitting of the levels with $M\neq 0$ and $K\neq 0$. The lowest eigenvalue E_{000} lies at -140 meV and it corresponds to the ground orientational level above the cation site, which is written in the free rotor basis such as:

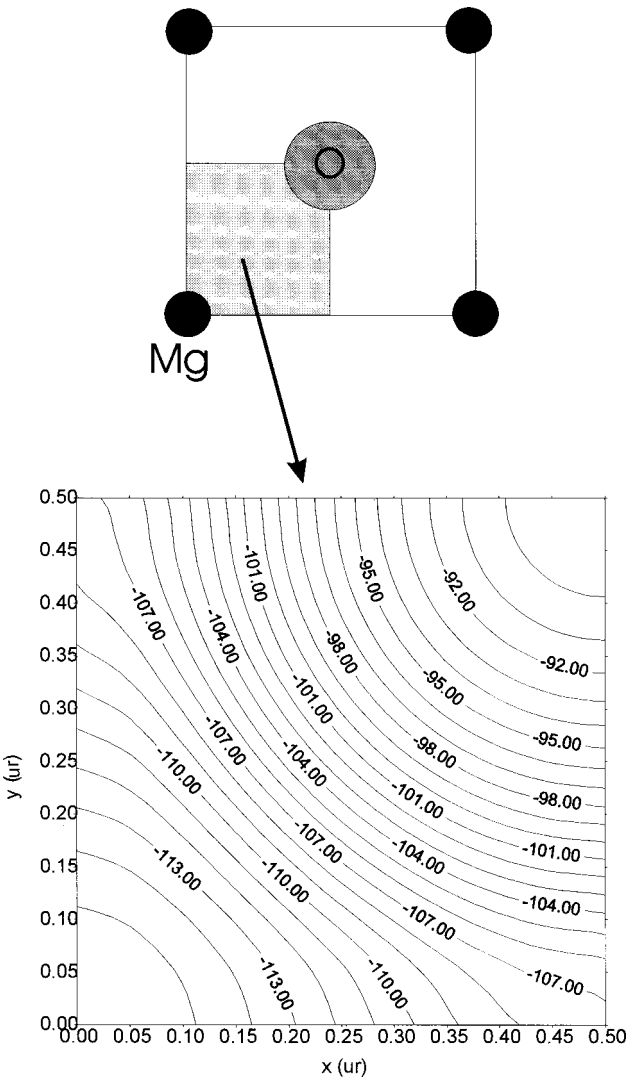

FIG. 2. Potential energy map for a free rotating CH_4 molecule above the MgO(100) surface. Energy in meV, distances in reduced unit of $a_s=2.98$ Å .

$$\begin{aligned}|j=0,m=0,k=0\rangle &= 0.621|000\rangle+0.151|100\rangle-0.185|200\rangle-0.395|300\rangle \\ &+0.365|30-3\rangle-0.365|303\rangle+0.163|40-3\rangle \\ &-0.163|403\rangle+\cdots\end{aligned} \tag{5}$$

As is expected the interaction of the molecule with the surface strongly mixes the free rotor states. As a result, the non-rotating, free CH_4 contribution [i.e., $(a_{000}^{000})^2$ in Eq. (3)] accounts to slightly less than 40%. In addition, the ground-state mixing mostly involves the $J=K=3$ states that contribute in total for slightly more than 40%. Such a symmetry of the ground ket indicates that the adsorption site corresponds to a hindered rotation of CH_4 with large amplitude motions around the tripod configuration.

Figure 4 shows the density of probability for finding the molecular axis orientation (tumbling θ motion) for various values of the internal rotation angle χ when the molecule is in its ground orientational state. Note that due to the internal symmetry of methane, we can limit our study to χ values

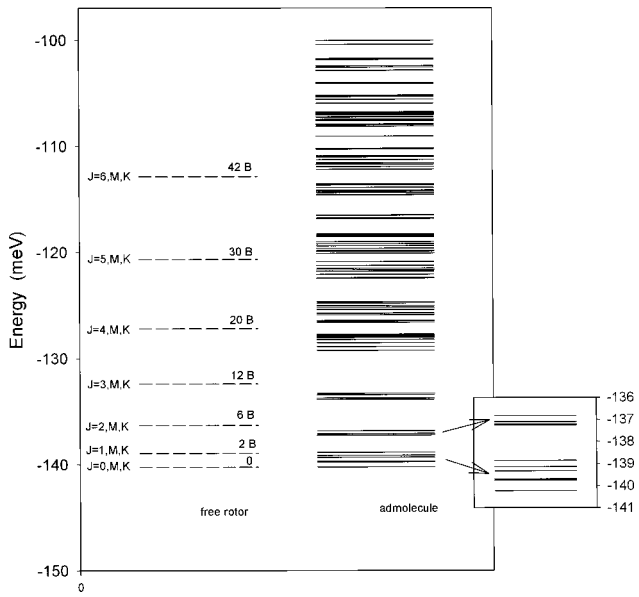

FIG. 3. Orientational levels scheme issued from the quantum study above the adsorption site. The insert shows the detail of the first orientational levels. For comparison, the free rotor scheme is given on the left hand side of the figure, as a function of the rotational constant *B*.

ranging between 0 and 60°. The large value of the full width at half maximum (about 40°) of the various curves indicates large amplitude motions around the most probable angle θ. The tripod configuration is clearly favored for χ values around 60° and $\theta \sim 70°$, while the dipod configuration occurs for χ values smaller than 30° and $\theta \sim 60°$. Let us mention that the classical (frozen) configurations for the tripod and dipod geometries would correspond to $\chi=60°$, $\theta=72°$ and $\phi=0°$, and to $\chi=0°$, $\theta=55°$, and $\phi=0°$, respectively. Thus, we can conclude that the orientation of CH_4 is no longer frozen as it is in the classical approach, and that the quantum result favors tripod and, in a less extent, dipod geometries.

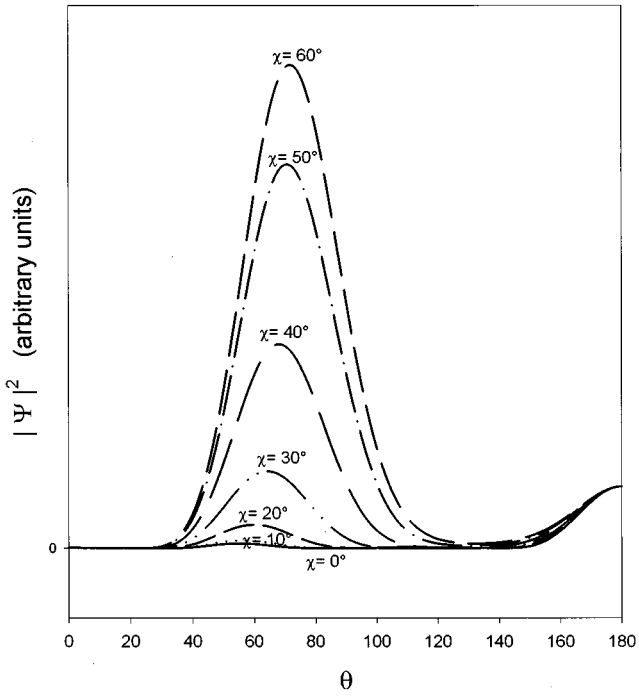

FIG. 4. Density of probability for finding the molecular θ orientation for various values of the internal angle χ and for $\phi=0°$, calculated in the ground orientational state $|j=0,m=0,k=0\rangle$, above the Mg site. Due to the site and molecule symmetries, we have restricted the range of χ values from 0 to 60°.

The excited orientational levels drawn in Fig. 3 stand very close together (more than 20 different states within 3 meV above the ground level). As a consequence, at finite temperature, a bunch of levels are populated and a better description of the final mean orientational map can be obtained after averaging over the canonical distribution of population, that is

$$\overline{V}_{MS}=\sum_{jmk}\frac{e^{-\Delta E_{jmk}/kT}}{Z}\langle jmk|V_{MS}|jmk\rangle, \tag{6}$$

where ΔE_{jmk} characterizes the energy difference between the $|jmk\rangle$ level and the ground state $|000\rangle$, and Z is the canonical partition function. The minimum of $\overline{V}_{MS}$ for the admolecule at $T=25$ and 70 K thus corresponds to energies equal to -144 and -145 meV, respectively, at the molecule-surface distance of 2.95 Å .

2. Monolayer

The Hamiltonian for the CH_4 monolayer is written as

$$H=\sum_i H_i+\sum_{ij} V_{MM}(\mathbf{R}_{ij},\mathbf{\Omega}_i,\mathbf{\Omega}_j) \tag{7}$$

where the first term characterizes the sum of the Hamiltonians H_i [Eq. (2)] over all the CH_4 admolecules and the second term accounts for the lateral interactions in the monolayer. R_{ij} is the instantaneous distance between the ith and jth CH_4 molecules. The solutions of the secular equation connected to the Hamiltonian H [Eq. (7)] are obtained in a way similar to the iterative process used for the single admolecule. We consider first a free rotor basis for the set of admolecules and calculate the mean lateral interaction in the ground orientational state $\Pi_i|J_i=0,M_i=0,K_i=0\rangle$ for the $(\sqrt{2}\times\sqrt{2})R45°$ layer structure. The value of the mean interaction $\langle V_{MM}\rangle$ per molecule is equal to -20 meV. This contribution represents less than 20% of the molecule-surface binding energy. When we average V_{MM} in the ground state of the quantum basis $\Pi_i|j_i m_i k_i\rangle=\Pi_i|0_i 0_i 0_i\rangle$ obtained after two iterations the mean value slightly changes to -23 meV. Therefore V_{MM} can be considered as a small perturbation with respect to V_{MS} which, within a first–order perturbation theory, modifies the eigenenergies without changing the eigenkets. The final basis $|j_i m_i k_i\rangle$ for each admolecule i is used, within the mean field approximation to calculate the mean orientational energy map $(\overline{V}_{MS}+\overline{V}_{MM})_i$ per molecule of the monolayer, and Eq. (6) is applied to take into account the finite temperature T in the range 25 to 70 K. The corresponding lateral interaction for a $(\sqrt{2}\times\sqrt{2})R45°$ monolayer containing one molecule per unit cell is equal to $\overline{V}_{MM}=-22$ meV.

TABLE I. Adsorption characteristics obtained in the classical and quantum approaches for the CH_4 monolayer

	Monopod	Dipod	Tripod	Free rotor	Hindered rotor	Experiment
z (Å)	3.40	3.03	2.74	3.18	2.95	
E_A (meV)	−119	−177	−228	−127	−152	−145±10
$\hbar\omega_x$ (cm^{-1})	25	36	55	31	40	
$\hbar\omega_y$ (cm^{-1})	25	36	55	31	40	
$\hbar\omega_z$ (cm^{-1})	77	106	129	88	95	60

Within these assumptions, the total orientational energy for the CH_4 monolayer adsorbed on MgO(100) is then equal to −162 meV per molecule. The final value of $(\overline{V}_{MS}+\overline{V}_{MM})_i$ is then used to calculate the vibrational frequencies of the molecular centers of mass parallel (x,y) and perpendicular (z) to the surface. This yields the values $\omega_x=\omega_y=40$ and $\omega_z=95$ cm^{-1}, which are much lower than the values obtained in the classical approach.

When the translational energy is taken into account, the resulting adsorption energy E_A per molecule in the monolayer defined as the energy required to bring an admolecule into its gas phase is equal to $E_A=-152$ meV. The characteristics of the CH_4 adsorption in the monolayer phase are given in Table I for the two approaches.

III. HELIUM SELECTIVE ADSORPTION SPECTRUM

Experiments focusing onto diffraction-mediated selective adsorption are quite useful in the study of atom scattering from physisorbed overlayers[29–31] since they bring indirect information on the geometry of the target (here the CH_4 monolayer) through the dynamical behavior of the atomic probe. Indeed, as the collider approaches the adlayer it can get trapped near the surface through a resonant diffraction transition, resulting in a sudden variation of the intensity of the specular or diffracted beams. A zeroth-order Hamiltonian representation of the scatterer motion perpendicular to the surface is used to derive the desired bound-state energies. In the Fourier expansion of the potential between the scatterer and the target the coupling due to non zero values of the G reciprocal vectors is neglected and the one-dimensional Schrödinger equation for the laterally averaged potential $V_{G=0}(z)$ is solved vs z, where z defines the position of the atomic collider with respect to the surface. In this model, the translational motion along the surface is assumed to be unaffected until the atom returns to the gas phase, i.e., no diffractive transition occurs in bound space. The atom is allowed to escape from the surface either by transferring its parallel energy into diffraction or through an inelastic process. Although this so-called ''free atom'' approximation is derived within a smooth surface assumption it has been applied in several studies of highly corrugated surfaces such as physisorbed overlayers. Jónsson *et al.*[30] have found that the position of isolated resonances is well predicted by the free atom model in the scattering of hydrogen atoms from a Xe monolayer on graphite. Gibson *et al.* have demonstrated that the selective adsorption data is extremely sensitive to the He interaction with overlayers of rare gases physisorbed on Ag(111).[31] A similar conclusion was obtained for Kr adsorbed on graphite by Larese *et al.* who showed that three body interactions can have a measurable effect on the determination of the bound-state energies.[29] The free atom model has also been invoked by Jung *et al.* to rule out the tripod equilibrium configuration of the CH_4 monolayer adsorbed on MgO(100) and probed by helium atoms.[10] The goal of the present section is to repeat He bound-state calculations for the methane-plated MgO system, on the basis of the new results described in Sec. II.

A. interaction potential

The physisorptive interaction between an impinging He atom labeled I and the methane-plated MgO system is written as[10,32]

$$V_I(\mathbf{r}_I)=V_{IM}(\mathbf{r}_I)+V_{IS}(z_I)+V_t(\mathbf{r}_I). \tag{8}$$

The first two contributions in Eq. (8) arise from two-body interactions with, respectively, the adlayer and the substrate. $\mathbf{r}_I$ defines the instantaneous position of the collider with respect to the target. Two additional terms, namely many-body corrections involving the scatterer and adsorbate pairs, and accounting for the substrate-mediated interaction with the adlayer are generally small. Although they appear negligible for this system they have been included to allow for a comparison with the results of Ref. 10. V_t represents the effect of thermal perpendicular vibrations of the adlayer, as determined from data of Sec. II. From Eq. (8) it is clear that the corrugation originates only from the dominant adlayer contribution V_{IM} and from its thermal correction V_t. Indeed, the trapped He atoms remain far enough from the substrate to consider that He–MgO interaction essentially amounts to a long-range van der Waals attraction V_{IS}, and does not yield appreciable corrugation.

The analytical expressions defining V_{IM}, V_{IS}, and V_t, are given by Eqs. (5)–(13) of Jung *et al.*[10] We have retained the same expressions and the same values of the relevant parameters. Yet, we consider in this paper the data obtained from both classical and quantum approaches in Sec. II. The dominant term V_{IM} is evaluated as a sum of pairwise interactions U, as

$$V_{IM}(\mathbf{r}_I)=\sum_I\left[U_0(\rho_I)+\sum_{p=3}^{4}U_p(\rho_I)T_p(\gamma_I,\phi_I)\right], \tag{9}$$

where the first sum is over the CH_4 lattice sites $\mathbf{R}_i$ and the second sum is over the successive anisotropic contributions of the gas phase He–CH_4 potential ($p=0$ corresponds to the isotropic part). (ρ_I,γ_I,ϕ_I) are the spherical coordinates of this potential. Like Jung *et al.*, we have used the potential of

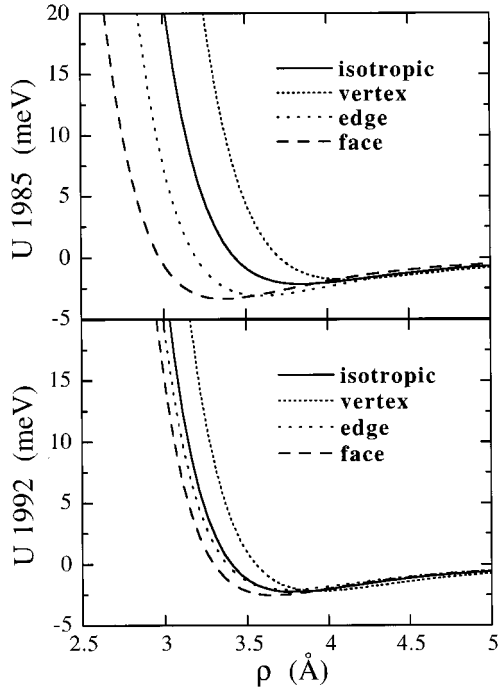

FIG. 5. Potential energy curves for He approaching CH_4 in the gas phase along the vertex, edge, and face orientations, and for the isotropic term. The upper (lower) panel pertains to the model of Buck *et al.* (Henkel *et al.*).

Buck *et al.* combining self-consistent field (SCF) calculations with damped dispersion coefficients[33], and, in addition, we have considered the semiempirical potential of Henkel *et al.*[34] These two gas phase potentials are displayed in Fig. 5 for the vertex, edge and face molecular orientations, that is for He approaching respectively, along a H–C bond, along the bisector of the angle between two H–C bonds, and along a C–H bond. The potentials are less repulsive as He closely interacts with more H atoms, respectively one, two, and three for the vertex, edge, and face approaches. The isotropic part of these potentials is also shown for comparison and it appears to be intermediate between the vertex and edge curves.

B. Bound-state energies

The diagonalization procedure is the same as in our previous study on He–(1×1) CO/NaCl,[35] ensuring that the eigenvalues are converged to better than 0.01 meV. The critical task is then to compute $V_{G=0}(z_I)$ accurately. This was carried out first for the conditions used by Jung *et al.*,[10] thus serving as a check that $V_I(\mathbf{r}_I)$ was properly evaluated. Upon comparison of our test results (not presented) with data of Ref. 10, the agreement is very good on the well depths and minimum positions as far as we match the tripod results of Jung *et al.* with the present monopod data. In the spherical harmonics expansion of the gas phase potential U, changing the sign in front of U_3 switches between the vertex and face orientations of CH_4. The relevance of this point shows up in the fact that Refs. 33 [Eq. (2)] and 34 [Eq. (14)] select opposite signs in front of U_3. However, the sequence depicted in Fig. 5 is based on the SCF findings and not on numerical subtleties.[33] Caution has been taken here to identify the vertex and the face orientations with respect to the interaction

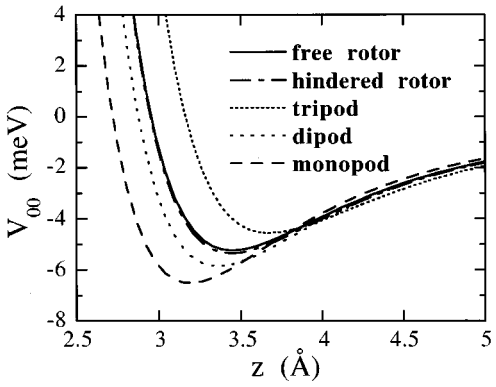

FIG. 6. Laterally averaged potentials for the tripod, dipod, monopod, and free rotor configurations of the adlayer, and for the quantum aproach, within the He–CH_4 interaction model of Buck *et al.*

properties, thereafter leading to the sequence in terms of adlayer configurations displayed in Fig. 6. With regard to the eigenvalues the agreement is fairly good for the ground state whereas there are some notable discrepancies on the weakly bounded states. The relative differences amount to about 10% on E_1 and to about 20% on E_2. Furthermore, we do not distinguish between the (010) and the (011) dipod orientations since they are found to produce the same $V_{G=0}(z_I)$ curves. Overall, despite some departures the comparison provides a valuable check of our numerical procedures.

Figure 6 depicts the laterally averaged potentials obtained for the tripod, dipod, monopod (classical approach), and free-rotor configurations, and for the quantum approach, with the respective z values determined in Sec. II and within the He–CH_4 interaction model of Buck *et al.*[33] Let us recall that the adsorption height varies from 2.74 to 3.40 Å as CH_4 reorients from tripod to monopod and it is equal to 2.95 Å for the orientational basis. The free rotor case amounts to selecting the isotropic He–CH_4 interaction at a CH_4/surface distance equal to 3.18 Å . Even if we have found that CH_4 cannot freely rotate at very low-surface temperature probed in the neutron experiments ($T\leqslant4$ K), the free rotor model is an asymptotic situation which may have a physical meaning at high temperatures, such as those probed by the HAS experimental range of 22–46 K.[10] Note also that the free rotor averaging treatment can be useful to account for tunneling exchange of one H up and one H down, analogous to CHD_3 on NaCl(100).[36] The unrealistic monopod configuration is also presented because it closes the sequence of curves that can be qualitatively compared with the gas phase potentials of Fig. 5. In order to facilitate the comparison the same line style has been selected from the most to the least repulsive potential curve. One could expect that the helium atom interacts strongly with one, two, or three H atoms on average, whenever the CH_4 layer is assumed in a tripod, dipod, or monopod adsorption configuration, respectively. This is actually the correct trend as the sequence of curves is monopod, dipod, quantum basis, free rotor, and tripod for the laterally averaged potential, consistent with the ordering face, edge, isotropic, and vertex in gas phase. The cases of more than one CH_4 molecule per surface unit cell need not be reported. Indeed, the resulting $V_{G=0}(z_I)$ curves are found

TABLE II. Well depth (D in meV), minimum position (z_{Im} in Å), and bound-state energy (E_n^I in meV) of the laterally-averaged potential obtained for the configurations discussed in Sec. II (Table I) and within the He–CH_4 interaction model of Ref. 33. Experimental energies of Ref. 10 are also indicated.

	Monopod	Dipod	Tripod	Free rotor	Hindered rotor	Experiments
D	6.51	5.83	4.56	5.23	5.34	
z_{Im}	3.19	3.36	3.67	3.44	3.44	
$\|E_0^I\|$	4.21	3.75	2.74	3.30	3.40	3.63 ± 0.18
$\|E_1^I\|$	1.44	1.27	0.85	1.07	1.13	1.25 ± 0.10
$\|E_2^I\|$	0.38	0.33	0.20	0.27	0.29	0.40 ± 0.08
$\|E_3^I\|$	0.07	0.06	0.03	0.05	0.05	

either identical by symmetry to the case of one molecule per cell, or negligibly differing, when averaging over all sites of the extended cell.

Table II lists the well depth (D) and minimum position (z_{Im}) of helium atom on the surface as well as the bound-state energies determined from each of the five configurations and the corresponding potentials drawn in Fig. 6. We see that the well depth is maximum for the monopod and minimum for the tripod, the dipod and quantum approach values being intermediate. The distance z_{Im} varies in an opposite sense and it is close for the dipod, free rotor, and quantum basis. As a consequence, the bound states for the dipod, free rotor, and quantum basis are rather close to each other while the monopod and tripod are clearly outside the range.

Table III presents the results stemming from the potential of Henkel *et al.*[34] for the same configurations of the monolayer. As can be seen in Fig. 5 this gas phase model is less anisotropic than the Buck's potential, especially in the well region, and it features much shallower wells. Hence, it is not surprising to get energy levels that depend more weakly on the molecule configuration and that are noticeably shifted up overall. Note more specially the consistency between the level scheme deduced from the dipod configuration and from the quantum basis.

IV. DISCUSSION

Two types of data are used to test the present approach: those that are deduced from direct investigations of the monolayer characteristics, namely the adsorption energy and the perpendicular vibrations of the CH_4 centers of mass, and those provided by the analysis of the collisional process of the monolayer by He atoms.

TABLE III. Well depth (D in meV), minimum position (z_{Im} in Å), and bound state energy (E_n^I in meV) of the laterally-averaged potential and within the He–CH_4 interaction model of Ref. 34.

	Monopod	Dipod	Tripod	Free rotor	Hindered rotor
D	5.27	5.26	4.74	5.05	5.16
z_{Im}	3.35	3.39	3.55	3.42	3.42
$\|E_0^I\|$	3.14	3.18	2.87	3.03	3.12
$\|E_1^I\|$	0.89	0.94	0.86	0.88	0.93
$\|E_2^I\|$	0.19	0.22	0.20	0.20	0.22
$\|E_3^I\|$	0.03	0.04	0.03	0.03	0.04

Table I shows that the adsorption energy per molecule E_A calculated within the quantum approach is much closer to the experimental value[16] than any other data resulting from classical frozen configurations (dipod, tripod ...) or from the free rotor model. The quantum description of the hindered rotor motion of CH_4 also produces the perpendicular frequency ω_z that is closer (with that of the free rotor model) to the experimental measurement. However, the agreement is not very good, indicating that the potential shape around equilibrium is probably not well described by the present expressions of the interactions between CH_4 and the MgO surface. This feature is also commonly observed for the physisorption of rare gas atoms and molecules on metals.[37]

The bound-state energies for helium atoms calculated from the Buck's[33] and Henkel's[34] potentials are given in Tables II and III, respectively. They can be compared to the experimental data[10] reported in the last column of Table II. When the Buck's potential is used we see that the monopod, tripod, and even free rotor models do not provide results consistent with experiment while the values of the energies calculated with the dipod configuration and the quantum approach are in satisfactory agreement with the experimental data. These two latter approaches lead also to results that are closer to experimental measurements than the other models when the Henkel's potential is considered, but the overall agreement is clearly less good than with the first potential.

The fact that none of the investigated configurations can perfectly meet the criteria of the experimental interpretation can have several origins. First, we can question the validity of the semi-empirical He–CH_4 description that does not reproduce the SCF repulsive anisotropy. Of course, this seems probable, but since we are not aware of any recent and accurate *ab initio* treatment of the full He–CH_4 interaction, this also remains hypothetical. In fact, an *ab initio* study of the dispersion forces[38] has been published in between Refs. 33 and 34. The leading dispersion coefficient was found to be $C_6 = 12.34$ a.u., a value that is intermediate between that of Ref. 33, $C_6 = 13.74$, and that of Ref. 34, $C_6 = 11.20$. This shows that none of the two gas phase potentials considered is really convincing. One could think of inserting the dispersion of Ref. 38 into one or the other model. However, in both cases a damping function is used to switch from the attractive to the repulsive behavior and the relevant parameters are closely connected to the fit of the measured differential cross sections of He scattering from CH_4.[33,34]

Another issue has to be raised as well, that is the free atom model. Jung *et al.*[10] have calculated some matrix ele-

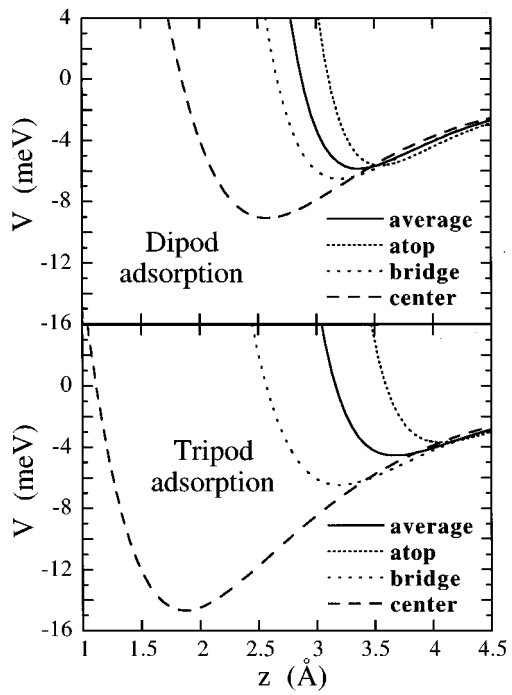

FIG. 7. Potential energy curves based on the He–CH_4 interaction model of Buck *et al.*, for He approaching the adlayer above the atop, bridge, and center sites, and for the laterally averaged term. The upper (lower) panel corresponds to the dipod (tripod) adsorption configuration.

ments of the higher-order Fourier expansion terms of Eq. (8) that are useful in a perturbation treatment of the free atom model to get the band structure of the bound states. They have done it for the free rotor assumption and found that the coupling matrix elements were quite large, consistent with the bumpiness of the potential. Indeed, the molecular specificity of the adlayer effects in an unusually large corrugation for He. The configuration deduced from the quantum approach has been found to lie much closer to the dipod configuration than to the tripod one. Figure 7 illustrates the corrugation of the CH_4 monolayer probed by He, within either the dipod (with $z_a = 3.03$ Å) or the tripod (with $z_a = 2.74$ Å) assumption and the gas phase model of Buck *et al.* The corrugation amplitude at the rise of the repulsive wall, i.e. $V = 0$, is roughly 1.3 and 2.5 Å in the dipod and tripod cases, respectively. These values reflect the difference between He approaching above either the atop or the center site. The largest anisotropy can be expected to occur for the tripod configuration since the gas-phase interaction is the most repulsive along the vertex approach as for He above the atop site, and the most attractive in the high-symmetry face approach, similar to He above the center site with four surrounding H atoms. Yet, one should not forget that the anisotropy is partially damped within either the free rotor model or the quantum description of the hindered rotor motion. Therefore, these two approaches provide a more adequate basis for the free atom model to give reliable data. If the frozen configurations are to be scrutinized, as indicated by the energy minimization calculations (classical approach), then the free atom model is certainly inadequate with respect to the huge anisotropy both in position and in well depth. The preceding tripod analysis yields the highest bound level whereas the deepest local well occurs for He approaching the tripod–CH_4 adlayer above the center site with $D_C = 14.68$ meV to be compared with $D = 4.56$ meV for $V_{G=0}$. Even though the anisotropy is partly damped with the semiempirical description of Henkel *et al.*, the site-dependent potentials vary similarly, with tripod well depth $D_C = 11.34$ meV to be compared with $D = 4.74$ meV for $V_{G=0}$. If the free atom model is to be invalidated not only are the calculated eigenvalues irrelevant but furthermore the experimental binding energies[10] are of little use as well since their derivation relies on the same basic assumption. By contrast, if the analysis in terms of quantum approach (free rotor or quantum basis) is more adequate, then certainly the free atom model should give reliable data.

In conclusion, we have extended a prior quantum treatment of the hindered rotor motion of H_2 admolecules[21] to that of CH_4 adsorbates involving a much more complex basis expansion. This description gives satisfactory agreement albeit not perfect either for the adsorbate characteristics or for the bound-state energies of He. This could indicate that the semiempirical potential describing the adsorbate–substrate interactions is not elaborated enough to account for the configurations obtained from *ab initio* potential calculations.[15,39] It is somewhat surprising that this semiempirical potential fails for such a simple system since it was demonstrated that no energy transfer and thus, no chemical effects, take place in the adsorption process of CH_4 on MgO. One reason might be that the system under study is not that simple since we have demonstrated that a quantum approach is required and since CH_4 is much more complex than H_2. One could think of some enhanced sensitivity of the investigated properties induced by the quantum behavior of CH_4. One could also think that full convergence has not been reached in our quantum approach. But the numerical iterative procedure used to calculate the orientational motions of CH_4 on the basis of potentials with distributed charges and sites is too time consuming to test this full convergence. The fact that the tripod symmetry prevails after two iterations in agreement with classical minimization, lets one hope that any subsequent iteration should only serve as a refinement. Anyway, regarding the symmetry of the trapped system, it is most probable that the molecule orientation should not favor an adlayer configuration close to the dipod one on the surface and that CH_4 should rather display large amplitude angular motions near the tripod equilibrium geometry. Let us note that, due to the T_d symmetry of CH_4, correlated χ and θ large amplitude angular motions favor instantaneous configurations that could be identified either to quasidipod or quasitripod geometries by the He or neutron scatterers.

Regarding the He-bound state investigation we have found that the frozen dipod configuration and the quantum hindered rotor model give similar energies. The quantum model is clearly more adequate for an analysis of the CH_4 structure with temperature since it leads to a nearly free rotation of the CH_4 molecules as soon as temperature increases to 20–30 K. Such a result is consistent with the data of inelastic neutron scattering[8] and with the interpretation of polarized infrared spectra.[17] Furthermore, the degeneracy removing of the orientational states, which rules out the fundamental orientational transition with energy equal to $2B$

=1.2 meV seems to be verified in recent results dealing with very low temperature orientational tunnelling spectroscopy experiments.[18] Indeed such a transition does not occur in the spectrum, in agreement with a hindered rotation of the admolecules, but the structures appearing close to the elastic peak are assigned by Larese[18] to proton tunneling for CH_4 molecules frozen in a dipod orientation. At this stage, we have not calculated the signals that would come from the orientational levels of the CH_4 molecules in the monolayer.

ACKNOWLEDGMENTS

C.G. and S.P. would like to thank Dr. P. Hoang for his numerical help in the quantum study of the adsorption characteristics. The Center d'Etudes et de Recherches Laser et Applications is supported by the Ministère chargé de la Recherche, the Région Nord/Pas de Calais, and the Fond Européen de Développement Economique des Régions.

*FAX: (33) 3 81 66 64 75.
Electronic address: claude.girardet@univ-fcomte.fr

[1] A. Thomy and X. Duval, J. Chim. Phys. Phys.-Chim. Biol. **67**, 1101 (1970).
[2] J.P. Coulomb, M. Bienfait, and P. Thorel, J. Phys. C **38**, 31 (1977).
[3] P. Thorel, J.P. Coulomb, and M. Bienfait, Surf. Sci. **114**, L43 (1982).
[4] J.P. Coulomb, K. Madih, B. Croset, and H.J. Lauter, Phys. Rev. Lett. **54**, 1536 (1985).
[5] M. Bienfait, J.P. Coulomb, and J.P. Palmari, Surf. Sci. **182**, 557 (1987).
[6] M. Bienfait, J.M. Gay, and H. Blank, Surf. Sci. **204**, 331 (1988).
[7] J.M. Gay, J. Suzanne, and J.P. Coulomb, Phys. Rev. B **41**, 11 346 (1990).
[8] J.Z. Larese, J.M. Hastings, L. Passell, D. Smith, and D. Richter, J. Chem. Phys. **95**, 6997 (1991).
[9] J.M. Gay, P. Stocker, D. Degenhardt, and H.J. Lauter, Phys. Rev. B **46**, 1195 (1992).
[10] D.R. Jung, J. Cui, D.R. Frankl, G. Ihm, H.Y. Kim, and M.W. Cole, Phys. Rev. B **40**, 11 893 (1989).
[11] D.R. Jung, J. Cui, and D.R. Frankl, Phys. Rev. B **43**, 10 042 (1991).
[12] A. Alavi, Mol. Phys. **71**, 1173 (1990).
[13] C. Girard and C. Girardet, Chem. Phys. Lett. **138**, 83 (1987); A. Lakhlifi and C. Girardet, J. Chem. Phys. **94**, 688 (1991).
[14] B. Deprick and A. Julg, Chem. Phys. Lett. **110**, 150 (1984).
[15] K. Todnem, K.J. Borve, and M. Nygren, Surf. Sci. **421**, 296 (1999).
[16] K. Madih, Ph.D. thesis, Université d'Aix-Marseille, Marseille, 1986.
[17] D. Wetter, Ph.D. thesis, Universität Hannover, Hannover, 1996.
[18] J.Z. Larese, Physica B **248**, 297 (1998).
[19] L.M. Quattrocci and G.E. Ewing, J. Chem. Phys. **96**, 4205 (1992).
[20] J. Heidberg, O. Schönekäs, H. Weiss, G. Lange, and J.P. Toennies, Ber. Bunsenges. Phys. Chem. **99**, 1370 (1995).
[21] S. Briquez, S. Picaud, C. Girardet, P.N.M. Hoang, J. Heidberg, and A. Voßberg, J. Chem. Phys. **109**, 6435 (1998).
[22] M. Sidoumou, V. Panella, and J. Suzanne, J. Chem. Phys. **101**, 6338 (1994).
[23] J.O. Hirschfelder, C.F. Curtiss, and R.B. Bird, *Molecular Theory of Gases and Liquids* (Wiley, New York, 1967).
[24] C. Girardet, S. Picaud, and P.N.M. Hoang, Europhys. Lett. **25**, 131 (1994).
[25] C. Girardet, P.N.M. Hoang, and S. Picaud, Phys. Rev. B **53**, 16 615 (1996).
[26] S. Picaud, C. Girardet, A. Glebov, J.P. Toennies, J. Dohrmann, and H. Weiss, J. Chem. Phys. **106**, 5271 (1997).
[27] D. Ferry, S. Picaud, P.N.M. Hoang, C. Girardet, L. Giordano, B. Demirdjian, and J. Suzanne, Surf. Sci. **409**, 101 (1998).
[28] G. Herzberg, *Molecular Spectra and Molecular Structures. II. Infrared and Raman Spectra of Polyatomic Molecules* (Van Nostrand, New York, 1966).
[29] J.Z. Larese, W.Y. Leung, D.R. Frankl, N. Holter, S. Chung, and M.W. Cole, Phys. Rev. Lett. **54**, 2533 (1985).
[30] H. Jónsson, J.H. Weare, T.H. Ellis, and G. Scoles, Surf. Sci. **180**, 353 (1987).
[31] K.D. Gibson, C. Cerjan, J.C. Light, and S.J. Sibener, J. Chem. Phys. **88**, 7911 (1988).
[32] S. Chung, N. Holter, and M.W. Cole, Phys. Rev. B **31**, 6660 (1985).
[33] U. Buck, K.H. Kohl, A. Kohlhase, M. Faubel, and V. Staemmler, Mol. Phys. **55**, 1255 (1985).
[34] M. Henkel, B. Pfeil, and W. Seidel, J. Chem. Phys. **96**, 5054 (1992).
[35] M.N. Carré, D. Lemoine, S. Picaud, and C. Girardet, Surf. Sci. **347**, 128 (1996).
[36] K.A. Davis and G.E. Ewing, J. Chem. Phys. **107**, 8073 (1997).
[37] J.E. Black and A. Janzen, Surf. Sci. **217**, 199 (1989).
[38] P.W. Fowler, P. Lazzeretti, and R. Zanasi, Mol. Phys. **68**, 853 (1989).
[39] A.M. Ferrari, S. Huber, H. Knözinger, K.M. Neyman, and N. Rösch, J. Phys. Chem. B **102**, 4548 (1998).